

Patterns in Wetland Microbial Community Composition and Functional Gene Repertoire Associated with Methane Emissions

Shaomei He,^a Stephanie A. Malfatti,^{a,c} Jack W. McFarland,^b Frank E. Anderson,^b Amrita Pati,^a Marcel Huntemann,^a Julien Tremblay,^a Tijana Glavina del Rio,^a Mark P. Waldrop,^b Lisamarie Windham-Myers,^b Susannah G. Tringe^a

DOE Joint Genome Institute, Walnut Creek, California, USA^a; U.S. Geological Survey, Menlo Park, California, USA^b; Lawrence Livermore National Laboratory, Livermore, California, USA^c

ABSTRACT Wetland restoration on peat islands previously drained for agriculture has potential to reverse land subsidence and sequester atmospheric carbon dioxide as peat accretes. However, the emission of methane could potentially offset the greenhouse gas benefits of captured carbon. As microbial communities play a key role in governing wetland greenhouse gas fluxes, we are interested in how microbial community composition and functions are associated with wetland hydrology, biogeochemistry, and methane emission, which is critical to modeling the microbial component in wetland methane fluxes and to managing restoration projects for maximal carbon sequestration. Here, we couple sequence-based methods with biogeochemical and greenhouse gas measurements to interrogate microbial communities from a pilot-scale restored wetland in the Sacramento-San Joaquin Delta of California, revealing considerable spatial heterogeneity even within this relatively small site. A number of microbial populations and functions showed strong correlations with electron acceptor availability and methane production; some also showed a preference for association with plant roots. Marker gene phylogenies revealed a diversity of major methane-producing and -consuming populations and suggested novel diversity within methanotrophs. Methanogenic archaea were observed in all samples, as were nitrate-, sulfate-, and metal-reducing bacteria, indicating that no single terminal electron acceptor was preferred despite differences in energetic favorability and suggesting spatial microheterogeneity and microniches. Notably, methanogens were negatively correlated with nitrate-, sulfate-, and metal-reducing bacteria and were most abundant at sampling sites with high peat accretion and low electron acceptor availability, where methane production was highest.

IMPORTANCE Wetlands are the largest nonanthropogenic source of atmospheric methane but also a key global carbon reservoir. Characterizing belowground microbial communities that mediate carbon cycling in wetlands is critical to accurately predicting their responses to changes in land management and climate. Here, we studied a restored wetland and revealed substantial spatial heterogeneity in biogeochemistry, methane production, and microbial communities, largely associated with the wetland hydraulic design. We observed patterns in microbial community composition and functions correlated with biogeochemistry and methane production, including diverse microorganisms involved in methane production and consumption. We found that methanogenesis gene abundance is inversely correlated with genes from pathways exploiting other electron acceptors, yet the ubiquitous presence of genes from all these pathways suggests that diverse electron acceptors contribute to the energetic balance of the ecosystem. These investigations represent an important step toward effective management of wetlands to reduce methane flux to the atmosphere and enhance belowground carbon storage.

Received 27 January 2015 Accepted 17 April 2015 Published 19 May 2015

Citation He S, Malfatti SA, McFarland JW, Anderson FE, Pati A, Huntemann M, Tremblay J, Glavina del Rio T, Waldrop MP, Windham-Myers L, Tringe SG. 2015. Patterns in wetland microbial community composition and functional gene repertoire associated with methane emissions. *mBio* 6(3):e00066-15. doi:10.1128/mBio.00066-15.

Editor Mark J. Bailey, CEH-Oxford

Copyright © 2015 He et al. This is an open-access article distributed under the terms of the [Creative Commons Attribution-Noncommercial-ShareAlike 3.0 Unported license](https://creativecommons.org/licenses/by-nc-sa/4.0/), which permits unrestricted noncommercial use, distribution, and reproduction in any medium, provided the original author and source are credited.

Address correspondence to Susannah G. Tringe, sgtringe@lbl.gov.

Wetlands cover about 5 to 8% of the earth's land surface (1) and provide important ecosystem services such as wildlife habitat, water purification, and flood control. As a major terrestrial carbon reservoir, estimated at 20 to 30% of the global soil carbon pool (2), wetlands play an important role in global carbon cycling, yet around the world wetlands are shrinking due to agricultural and industrial development and urbanization (3), releasing stored carbon into the atmosphere and accelerating climate change.

In the Sacramento-San Joaquin (SSJ) Delta area, California, historic freshwater tidal marshes were drained and converted to

agriculture for their fertile organic-rich soils between the late 19th and early 20th centuries (4). Substantial land surface subsidence has since occurred, largely due to accelerated microbial oxidation of peat as drainage increased soil aeration (5), causing significant carbon loss to the atmosphere and imposing a risk of levee failures in the SSJ Delta (6). One potential means to mitigate these risks is to restore these historical wetlands, as waterlogged anoxic conditions are expected to slow microbial decomposition and favor peat accumulation from wetland plant detritus. To evaluate the long-term carbon storage rates and land subsidence reversal potential of reestablished wetlands, in 1997 the U.S. Geological Survey

(USGS) and the California Department of Water Resources (DWR) started a pilot-scale restoration project on Twitchell Island in the SSJ Delta with managed hydrology. Data collected from 1997 to 2006 demonstrated that rapid peat accretion and land surface elevation were achievable, with an average rate of ~ 4 cm/year (7).

In addition to reversing land subsidence, the high primary production and low decomposition rates in restored wetlands may result in a net atmospheric carbon dioxide (CO_2) sequestration, allowing them to act as “carbon farms.” However, one major concern is the emission of methane (CH_4), a common decomposition end product in anoxic environments when terminal electron acceptors are depleted. CH_4 is a potent greenhouse gas (GHG) with a 100-year global warming potential 25 times higher than that of CO_2 , and natural wetlands contribute ~ 20 to 39% of global CH_4 emissions (8), making them the largest nonanthropogenic source of atmospheric CH_4 . When CH_4 emission is large enough to counterbalance the CO_2 captured by primary production, a wetland may effectively change from a GHG sink to a GHG source (9). CH_4 and CO_2 flux data collected during the first 6 years (1997 to 2003) from the pilot-scale restoration wetlands on Twitchell Island indicated that these wetlands could mitigate carbon loss and even become a net GHG sink (10). However, their long-term carbon storage potential and GHG budget are the subject of ongoing investigation.

Net CH_4 emission is governed by production, oxidation, and transportation and varies widely among wetlands due to differences in vegetation, soil type, pH, organic carbon composition, water chemistry, hydrology, and climate, as discussed in reviews (11–14). In wetland ecosystems, microbial communities play an important role in governing carbon flux, as dead plant biomass is either stored as peat or decomposed through microbial activities. Under conditions depleted of oxygen and other electron acceptors, methanogenic archaea use CO_2 or small organic compounds (e.g., acetate and methylamines) as the terminal electron acceptor to produce CH_4 . The amount of carbon diverted to methanogenesis can be influenced by anaerobic respiration processes dependent on nitrate, manganese(IV), iron(III), and sulfate, which commonly occur in wetland environments. The produced CH_4 can be consumed by methanotrophs, which generate energy through oxidation of CH_4 with oxygen at the water-sediment interface or rhizosphere, where both CH_4 and oxygen are available. All these microbial processes can affect the net production and release of CH_4 .

Variations in peat accretion within the pilot-scale restored wetland on Twitchell Island have been attributed to the hydraulic design (a gradient from inlet to outlet), and we expected to also observe biogeochemical gradients associated with the hydrology. Therefore, we hypothesized that peat microbial community composition and functions, as well as CH_4 emission, would exhibit patterns associated with the biogeochemical gradients due to distance from the inlet and proximity to plant roots. To test this, we collected biogeochemical data, evaluated CH_4 emission from different sites and sample types within the wetland, and applied a high-throughput sequencing approach to characterize peat microbial community composition and functional profiles, focusing on the microbial populations and processes influencing CH_4 flux. We aimed to identify community patterns, indicator species, genes, and pathways that are associated with biogeochemical variables and CH_4 emission along the gradient.

RESULTS AND DISCUSSION

Site biogeochemistry. We selected sites with a decreasing proximity to the inlet and differing rates of peat accretion: an “inlet” site with low accretion (A), a “transitional” site with intermediate accretion (B), and two “interior” sites with high accretion (C and L) (7) (see Fig. S1 in the supplemental material).

From the inlet to interior sites, pH, sulfate, nitrate, and dissolved oxygen (DO) at the standing water-peat interface decreased, and soluble iron (Fe) and manganese (Mn) increased in February (Fig. 1a and b). Increasing solubilization of Fe and Mn results from solid-phase Fe(III) and Mn(IV) reduction (12). These physicochemical patterns across sites were similar for August (Fig. 1d and e), although weaker than those in February. The pH of river water inputs was ~ 7.7 and decreased from the inlet to interior sites (from 7.0 to 6.5 in February and from 6.5 to 6.2 in August), likely due to anoxic decomposition of plant detritus, which releases carbonic, fulvic, humic, and other organic acids (15). River water had a DO concentration of ~ 8 mg/liter and was the primary source of nitrate, sulfate, and oxidized Fe (10). The observed decreases in electron acceptors in conjunction with increases in reduced Fe and Mn suggest that a variety of electron acceptors were being consumed along the water passage, although at these concentrations nitrate is predicted to be the most energetically favorable electron acceptor. Additionally, interior sites (“backwater” areas) experienced less hydraulic mixing and chemical exchange with river water than did the inlet site, which likely further decreased the influx of electron acceptors to the interior.

At the inlet site, with increasing peat depth, we observed decreases of nitrate and sulfate and increases of soluble Fe(II) and Mn(II) for both seasons (Fig. 1c and f), indicating that the environment becomes more reduced with depth as is common for wetland pore waters (16). Other sampling sites displayed similar depth-dependent redox gradients (see Fig. S1 in the supplemental material).

CH_4 flux. From laboratory incubations of February samples, statistically significant differences in CH_4 production were observed among the three sites (Fig. 2a). As the incubations were conducted in airtight jars, CH_4 oxidation was expected to be minimal. The lower net production of CH_4 from samples collected at the inlet than from the transitional or the interior site suggests lower methanogenic potential at the inlet site.

In August, CH_4 flux was monitored *in situ* using static chambers. Significantly lower CH_4 emissions were observed at the inlet and transitional sites than at the interior site (Fig. 2b). Although CH_4 emission at the inlet site averaged lower than that at the transitional site, this difference was not significant. Overall, both February laboratory incubation and August on-site measurement suggest similar variation in CH_4 emission among sites, which was lower at the inlet and higher at the interior.

Microbial community composition. Wetland microbial communities as assessed by 16S rRNA gene sequencing harbored members of numerous phyla and averaged a Shannon diversity index of 5.8, higher than the average Shannon index of 5.0 in the adjacent cornfield soil. Wetland microbial community composition was also different from that of the adjacent cornfield soil. Specifically, wetlands displayed higher abundances of *Proteobacteria*, *Chloroflexi*, *Bacteroidetes*, and *Euryarchaeota*, particularly *Methanomicrobia* (see Fig. S2 in the supplemental material), and this is consistent with the expectation that after inundation, soil

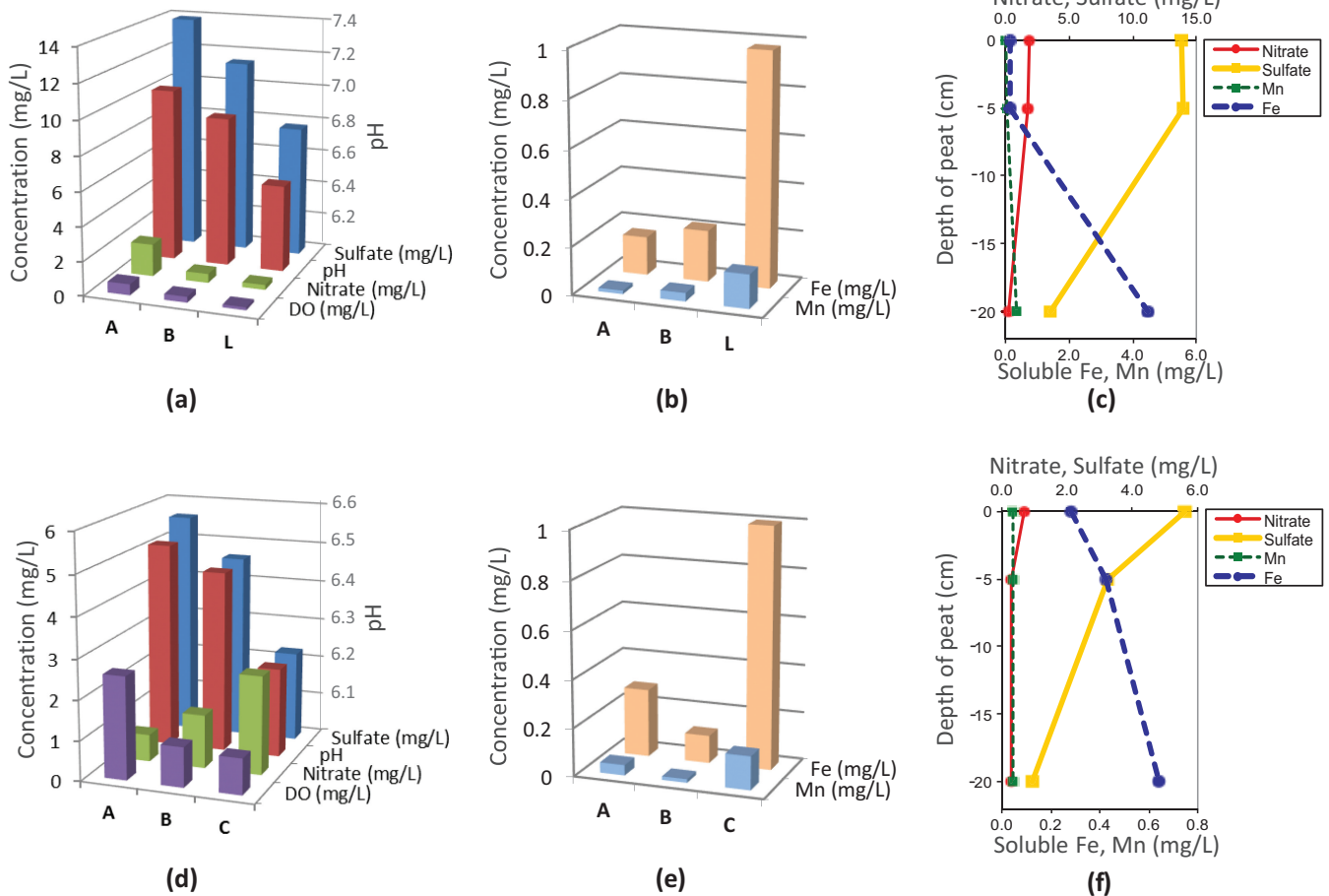


FIG 1 Physicochemical gradients across sites A (inlet), B (transitional), and L/C (interior) at the standing water-peat interface in February (a and b) and August (d and e) and peat pore water chemical profiles along the depth at site A (inlet) in February (c) and in August (f). Iron (Fe) and manganese (Mn) were measured as the soluble fraction, which is mostly as Fe(II) and Mn(II), respectively, under *in situ* pH.

environments become more anoxic and therefore enriched in these phyla commonly found in anoxic environments (17).

At the operational taxonomic unit (OTU) level, community composition was more influenced by sample site and sample type (bulk peat versus plant rhizome) and less influenced by depth or

season (Fig. 3). Among February samples, the largest site-associated community difference was between the inlet and the interior site, with communities from the transitional site in between on the nonmetric multidimensional scaling (NMDS) plot (Fig. 3a). A similar site-associated community pattern was observed for August samples, but communities from the transitional and the interior sites were not significantly different (Fig. 3c), which may be attributed to the weaker site chemical gradients in August than in February (Fig. 1). Site-associated community differences were also revealed on the correspondence analysis biplot (see Fig. S3 in the supplemental material), where the environmental variables, particularly the electron acceptor availabilities (such as DO, sulfate, and nitrate), were strongly correlated with the community patterns.

Sample type also influenced microbial communities. Tule and cattail rhizomes contain microbial communities distinct from bulk peat communities (Fig. 3b and d), likely reflecting the microenvironmental and/or chemical differences between rhizomes and bulk peat. Bulk peat is anoxic and mainly comprised of decomposed plant material. However, wetland vascular plants transport oxygen to roots to support root aerobic respiration and oxidation of Fe(II) and Mn(II) (18); oxygen leakage from roots and

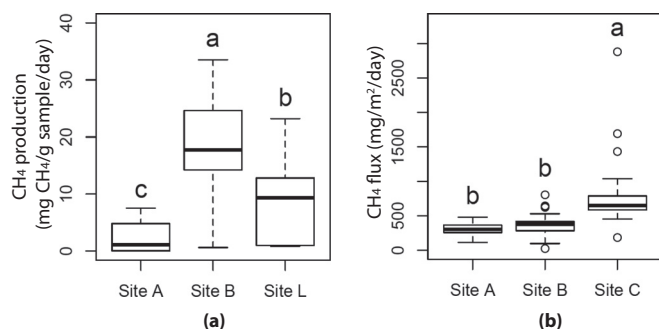


FIG 2 Box plot of net CH₄ production from the laboratory incubation of samples collected in February (a) and box plot of noon CH₄ flux measured on-site during August sampling (b) for the different sites. Letters within the plots (“a,” “b,” and “c”) indicate groups by Duncan’s new multiple range test. Sites within the same group are not significantly different.

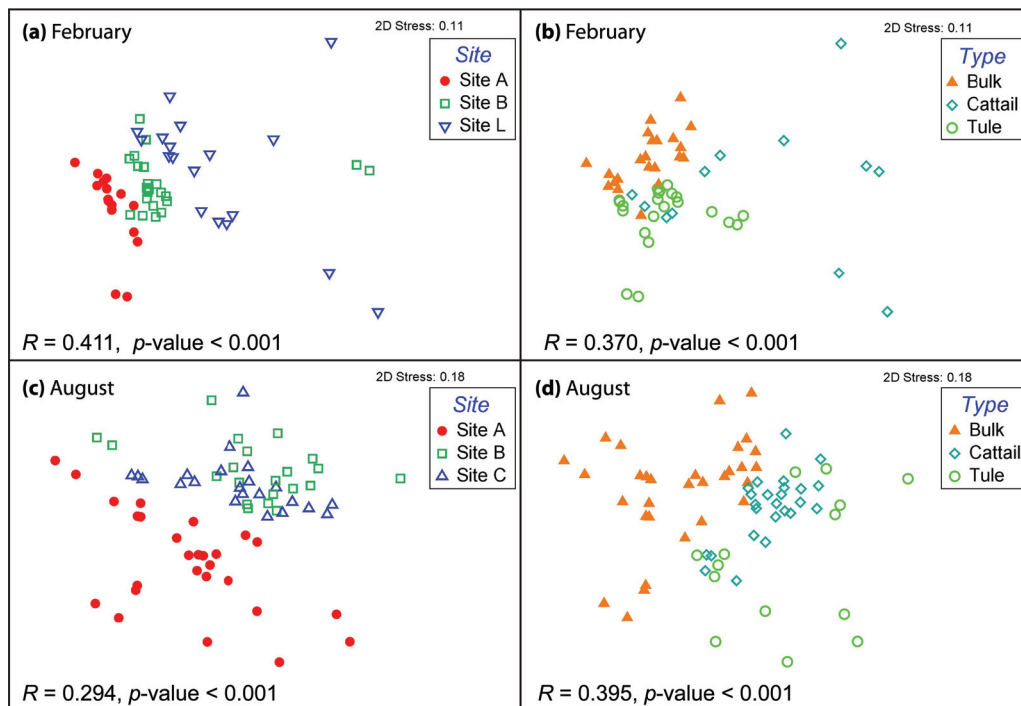


FIG 3 Nonmetric multidimensional scaling (NMDS) analysis of microbial communities based on relative abundance of OTUs for February (a and b) and August (c and d) wetland samples. (a and c) Data points colored by sample site; (b and d) data points colored by sample type. The indicated ANOSIM R statistics and PerMANOVA P values for panels a and c and for panels b and d were based on the comparisons among sample sites and among sample types, respectively.

rhizomes can cause elevated oxygen levels immediately surrounding roots and rhizomes (19). In addition, labile carbon is released from plant roots as exudates (20), leading to elevated levels of exudate-derived metabolites, such as acetate, in the rhizosphere (21). Further, plant-microbial interactions, including symbioses, can select for unique microbial communities within the rhizosphere (22).

Community differences between low- and high-CH₄-flux sites. Over 100 OTUs are differentially represented between the low-CH₄-flux communities (from the inlet site) and the high-CH₄-flux communities (from the transitional and the interior sites) for February samples (see Table S1A in the supplemental material). Of particular interest are methanogens, which are anaerobic archaea belonging to the *Euryarchaeota*. Three microbial pathways have been found for methanogenesis depending on substrates used: hydrogenotrophic (from H₂ and CO₂), methylotrophic (from methylated compounds), and acetoclastic pathways (from acetate) (23). Consistent with the higher CH₄ flux observed in transitional and interior sites, we observed higher relative abundances of methanogenic OTUs at these two sites (see Table S1A and Fig. S4a), including OTUs belonging to the hydrogenotrophic *Methanoregula* and *Methanobacterium* genera (23–25), the metabolically versatile *Methanosarcina* genus that can use all three methanogenic pathways (23), and the acetoclastic specialist *Methanosaeta*, whose cultivated representatives use only acetate and have a high affinity for acetate compared to that of *Methanosarcina* (26).

In contrast, many proteobacterial OTUs were more abundant at the inlet site (see Table S1A and Fig. S4b in the supplemental material). These include OTUs classified as *Dechloromonas*, many members of which are able to use nitrate as an electron acceptor;

Desulfobacteraceae, a sulfate-reducing family belonging to the *Delataproteobacteria* (27); *Thiobacillus* (16S rRNA V8 region 100% identical to *Thiobacillus denitrificans*), an obligate autotroph that can couple thiosulfate oxidation to denitrification (28, 29); and *Geobacter*, a genus encompassing species capable of reducing insoluble Fe and Mn oxides in soils and sediments (30). Higher representation of these OTUs at the inlet site corresponds well with the higher availability of sulfate, nitrate, Fe(III), and Mn(IV) at the inlet than at transitional or interior sites and likely contributes to lower methanogenesis and higher carbon mineralization via alternative terminal electron-accepting pathways. The coexistence of all these OTUs also suggests that a variety of electron acceptors are being used at this site, possibly within spatial and temporal microniches where electron acceptor availability is not accurately represented by bulk biogeochemistry.

Community differences between bulk peat and rhizomes. A number of alphaproteobacterial OTUs had higher relative abundance in rhizome samples (see Table S1B in the supplemental material), particularly in the order *Rhizobiales*, which includes nitrogen-fixing symbionts of plant roots and methanotrophs in the family of *Methylocystaceae*, such as *Methylosinus* (see Fig. S4c), a type II aerobic methanotroph (31, 32), which may find a niche at the rhizome surface, where low levels of oxygen are present. A number of methanogenic OTUs classified as *Methanobacterium*, *Methanosarcina*, *Methanosaeta*, and the family *Methanospirillaceae* were also more abundant in rhizomes, despite the overall lower number of methanogens (see Table S1B and Fig. S4c). Similarly, Cadillo-Quiroz and colleagues found higher relative abundances of *Methanosarcina* and *Methanosaeta*, the only two genera known to include members capable of using acetate for methanogenesis, in rhizosphere than in bulk peats (33), a pattern likely

linked to root exudation of acetate (21). Though methanogens are often regarded as strict anaerobes, oxygen is present near the rhizome (19), and so methanogens found on rhizomes must be able to tolerate oxygen. Indeed, Kiener and Leisinger (34) determined that some members of *Methanosarcina* and *Methanobacterium* are able to survive after an exposure to oxygen. In addition, *Methanosarcina* was found to be able to produce CH₄ even under oxic conditions, and its catalase genes were actively transcribed for oxygen detoxification (35).

OTUs more abundant in bulk peats include those classified as *Methanoregula*, *Crenarchaeota* C2 group, *Bacteroidales*, and *Thermodesulfovibrionaceae* (see Fig. S4d in the supplemental material). Previously, *Methanoregula* was also found to be more abundant in bulk peats than in rhizosphere and was the dominant methanogen in bulk peats (33). Members of *Methanoregula* are hydrogenotrophic methanogens (24, 25) and sensitive to even trace amounts of oxygen (25) and therefore are more likely to occur in bulk peats than under the microaerobic conditions surrounding rhizomes and roots. The *Crenarchaeota* C2 group, also known as rice cluster IV (36), is a deeply branched lineage initially identified from lake and marsh sediments (37) and has since been found in many anoxic environments, including sediment, soil, rice paddies, and anaerobic digesters (38). No cultured representative is available for this group, and their physiology is yet to be investigated.

Interspecies interactions. Interspecies interactions have the potential to affect wetland belowground processes through co-metabolic or syntrophic interactions. We explored potential interspecific interactions using correlation and network analyses (see Table S2A and B and Fig. S5 in the supplemental material). Methanogen OTUs were positively correlated with OTUs belonging to *Planctomycetes* and *Firmicutes* (particularly *Clostridia*), presumably due to methanogens' consumption of the carbohydrate fermentation products (e.g., acetate and hydrogen) generated by these populations. A number of methylotrophic alphaproteobacterial OTUs and a few *Syntrophaceae* OTUs in the *Deltaproteobacteria* co-occurred with methanogen OTUs. Methanogens were negatively correlated with many OTUs in *Proteobacteria* and *Nitrospirae* (especially *Thermodesulfovibrionaceae*), which contain anaerobic respiring populations. In total, there are 1,019 positive and 286 negative pairs of significant correlations among the analyzed OTUs. Interestingly, about one-third of the positive correlations were between OTUs in the same phylum, whereas only 3% of negative correlations occurred within the same phylum. For example, 26 pairs of methanogen OTUs were positively correlated, yet no negative correlations were found among methanogens. This indicates that species with the same functional guild tend to co-occur and may suggest that habitat filtering is a strong factor shaping microbial communities in this carbon- and nutrient-rich but electron-acceptor-poor environment.

Functional gene abundance profiles by metagenomics. Metagenome sequencing was conducted on 11 selected samples collected from the surface 0- to 12-cm peats in February, including different combinations of sample site and type, and two additional samples from a replicate core at site B, because a large variation of community composition was observed between the duplicate cores at this site. At least 52 Gb of sequence data was generated from each site. However, fewer than 10% of reads assembled into contigs of >200 bases in length for most samples (see Text S1A in the supplemental material), which reflects the high complexity of

wetland peat microbial communities. Indeed, under comparable sequencing efforts, the percentage of reads assembled was inversely correlated to the Shannon diversity index (*H*) of microbial communities estimated by 16S rRNA gene analysis (see Text S1A). Therefore, to best analyze the data, the assembled contigs and unassembled reads were both used for gene prediction and functional annotation, with the abundance of each contig adjusted by its read depth (fold coverage) for quantitative analyses. Genes and pathways involved in microbial processes in wetland peats, such as lignocellulose degradation, fermentation, anaerobic respiration, and production and oxidation of CH₄, were present in each metagenome as expected.

We used gene-centric analysis to reveal major differences in community functional profiles. The equal representation of housekeeping clusters of orthologous groups (COGs) among metagenomes indicates that bias associated with the average genome size in different samples was minimal and thus verifies the comparability of these metagenomes (see Text S1B in the supplemental material). Gene families involved in CH₄ metabolism, denitrification, dissimilatory sulfate reduction, dissimilatory metal reduction, nitrogen fixation, and hydrogen production and consumption were among the differentially represented gene families among sample sites and types. These are important functions generally found in wetland peats and are relevant to the biogeochemistry measurements that we collected. Therefore, we focused on gene families in these pathways, and a heat map was generated for these gene families to show their distribution patterns (Fig. 4).

Metagenomes from the interior site had the highest relative abundance of genes in methanogenesis pathways, consistent with higher CH₄ emission and higher abundance of methanogen OTUs at the interior site than at the inlet site. Metagenomes from the inlet site, on the other hand, had the highest representation of genes involved in dissimilatory sulfate reduction, denitrification, and metal reduction. Unlike the [NiFe] hydrogenase genes (pfam00374), the iron-only hydrogenase genes (pfam02256 and pfam02906) increased from the inlet to the interior site, suggesting that the environment became more fermentative and that more hydrogen was likely produced from fermentation through the iron-only hydrogenases in the interior site. As observed in the community composition data, the replicate cores from the transitional site (B1 and B2) showed large differences in functional gene abundance profiles (Fig. 4). Nevertheless, the abundance patterns of genes in these anaerobic respiration pathways are consistent with the chemical gradients and the differentially represented OTUs among these sites. Such functional gene distributions have not, to our knowledge, been previously demonstrated in wetland environments.

Nitrogenase genes required for nitrogen fixation were more abundant in rhizomes than in bulk peats, consistent with the over-representation of nitrogen-fixing *Rhizobiales* OTUs in rhizome samples from the 16S rRNA gene data. Similar to the nitrogenase gene pattern, genes involved in aerobic oxidation of CH₄ were more abundant in rhizomes than in bulk peats, reflecting the availability of oxygen near rhizomes and consistent with the over-representation of aerobic methanotrophs in rhizome samples from 16S rRNA gene analysis. The pattern of genes in CH₄ oxidation supports the idea that the oxygen leakage from roots and rhizomes creates a niche for aerobic methanotrophs to oxidize CH₄ to CO₂, thereby mitigating CH₄ emissions (39, 40). Because diffusion and gas-bubble ebullition through the water column

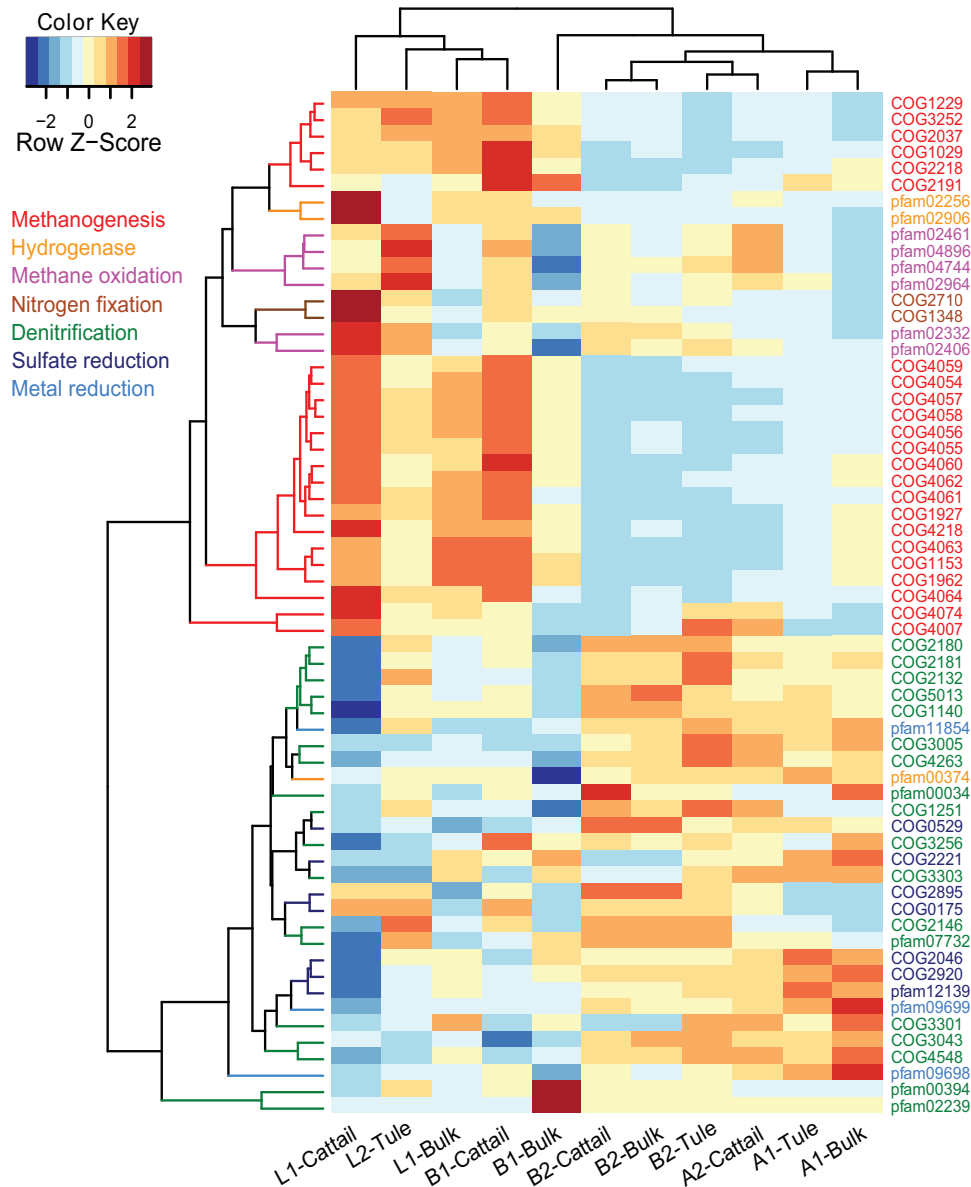
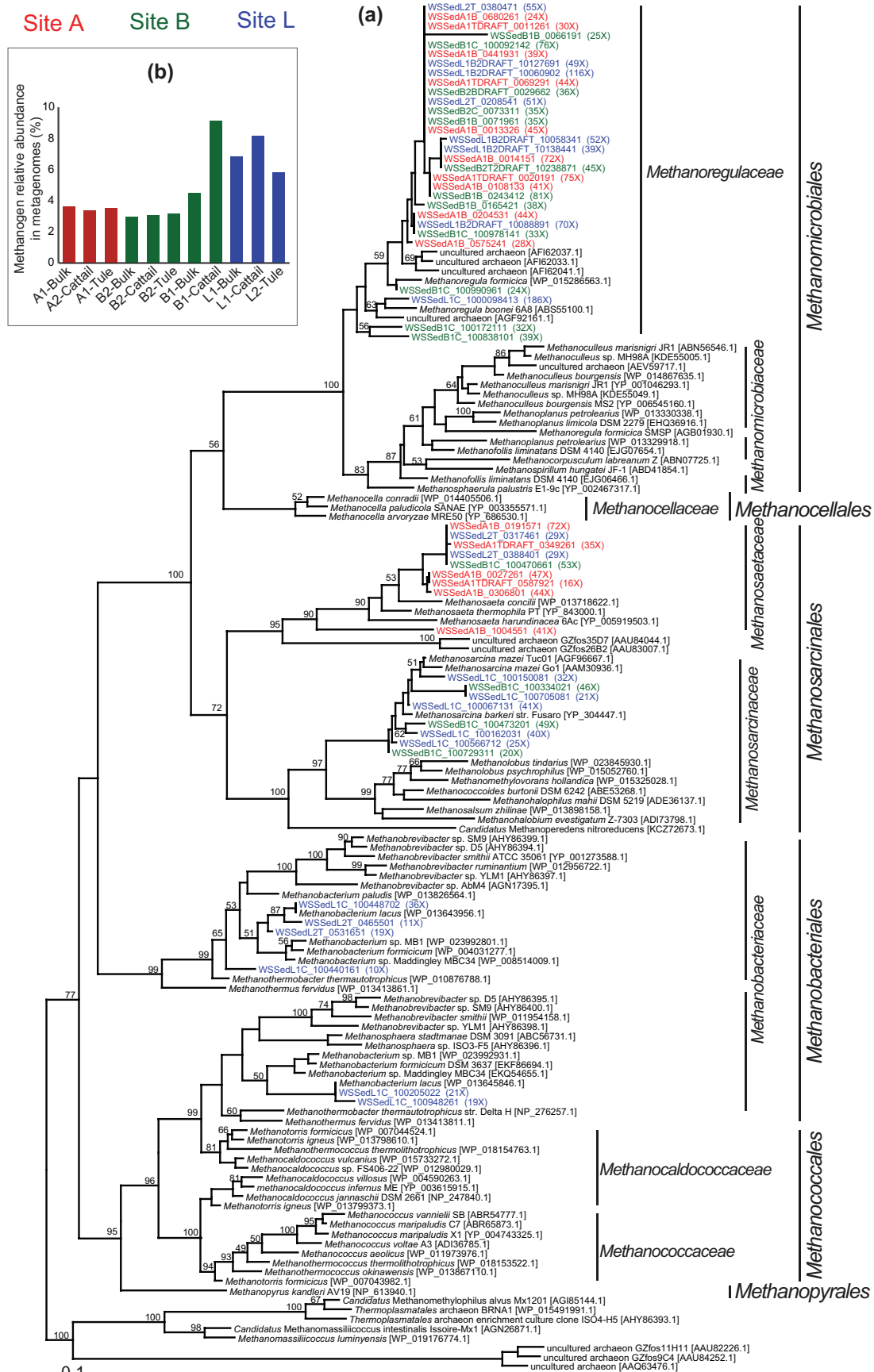


FIG 4 Heat map of gene families in important pathways generated with R and its “gplots” package, using the odds ratios between an individual metagenome and the combined average. Note that there are no COGs and Pfams specific for nitrite reductase genes *nirK* and *nirS*. As pfam02239 and pfam00034 are domains constituting *nirS* and COG2132, pfam00394, and pfam07732 are domains constituting *nirK*, we included them in this heat map, but note that they can also be components of some other redox genes.

typically contribute a minor proportion to CH₄ emission from wetlands compared to plant aerenchyma transport (10, 41), methanotrophs associated with plant roots and rhizomes can be a mitigating barrier that significantly reduces wetland CH₄ emission.

Diversity and distribution of methanogens. The genes encoding methyl coenzyme M reductase (MCR), which catalyzes the terminal step in methanogenesis, are functional markers of methanogenesis, and the gene for its subunit A, *mcrA*, is often used as a methanogen phylogenetic marker. We performed phylogenetic analysis using metagenome *mcrA* sequences from the assembled part, presumably derived from abundant methanogen populations in this wetland (Fig. 5a). All analyzed metagenome

mcrA sequences were affiliated with *Methanomicrobiales*, *Methanobacteriales*, and *Methanosarcinales*, spanning three out of the six major orders of known methanogens. The *Methanoregulaceae* family within *Methanomicrobiales* harbors more than half of metagenome *mcrA* sequences, some of which have high coverage (e.g., >50×). Particularly, an *mcrA* gene closely affiliated with *Methanoregula boonei* 6A8 has a very high coverage (i.e., 186×), which allowed the recovery of a near-complete genome of the methanogen containing it (data not shown). This genome has only the hydrogenotrophic methanogenesis pathway and lacks the methylotrophic pathway and the *hdrDE* genes needed for growing on acetate, confirming it as a hydrogenotrophic specialist. As members of *Methanomicrobiales* and *Methanobacteriales* are mostly hy-



drogenotrophic (23–25), their abundant presence suggests the importance of hydrogenotrophic methanogenesis in this wetland.

Among *Methanosarcinales*, the acetoclastic specialist genus, *Methanosaepta*, mainly contains sequences from site A, and the metabolically versatile genus, *Methanosarcina*, exclusively contains sequences from cattail rhizomes on sites B and L. The *Methanobacteriaceae* branch within the *Methanobacteriales* is represented only by rhizome samples from site L. These site- and type-associated methanogen distribution patterns remain even when we included additional shorter sequences from wetland metagenomes (data not shown). The type-associated patterns likely reflect acetate and oxygen availabilities as discussed in the above 16S rRNA gene analysis session.

We estimated the relative abundance of methanogens and several other functional guilds in the community by comparing their specific functional marker gene abundance to general single-copy housekeeping genes, using their length-normalized abundances (see Text S1C in the supplemental material for details on the normalization method). We expect this method to be much less biased than traditional PCR-based quantification, which is subject to PCR bias and depends on the design of functional gene and housekeeping gene primers inclusive enough for different taxa. To validate this method, we compared methanogen estimates by relative abundance of *mcr* genes against the estimates by 16S rRNA gene amplicon sequencing and by the classification of 16S rRNA gene reads in the metagenomes (42) (see Text S1D for details). We demonstrate that the estimate by metagenome *mcr* was very comparable to the estimate by metagenome 16S rRNA genes and was more quantitatively accurate than 16S rRNA gene amplicon sequencing. The estimated methanogens ranged from 2% to 10% of the total community and were highest at the interior and lowest at the inlet (Fig. 5b).

Diversity and distribution of methanotrophs. Methanotrophs use methane as a sole carbon and energy source and can be classified as type I (belonging to *Gammaproteobacteria*) and type II (belonging to *Alphaproteobacteria*) methanotrophs (43). For example, these types differ in carbon assimilation pathways, cell morphology, and ultrastructure. In addition, a verrucomicrobial methanotroph (44) and a nitrite-dependent anaerobic methane oxidizer, “*Candidatus* *Methylomirabilis oxyfera*” in candidate division NC10 (45), were also reported. The first step in methane oxidation is catalyzed by methane monooxygenase (MMO), which has two forms: a particulate membrane-bound form (pMMO) and a soluble cytoplasmic form (sMMO). Nearly all methanotrophs (with some exceptions such as *Methylocella*) possess pMMO, whereas sMMO is present in only a few methanotroph genera (32, 46). The alpha subunits of pMMO (*pmoA*) and sMMO (*mmoX*) genes are often used to study methanotroph phylogeny (32).

To reveal the diversity of methanotrophs, we first constructed a *pmoA* phylogenetic tree (Fig. 6a). The majority of wetland *pmoA* genes were affiliated with *Methylocystis* and *Methylosinus* within *Methylocystaceae* (type II), and some were affiliated with *Methylococcaceae* (type I). No sequence was affiliated with *Verrucomicro-*

bia or “*Ca. Methylomirabilis oxyfera*” (tree not shown), and this was confirmed by blasting *Verrucomicrobia* and “*Ca. Methylomirabilis oxyfera*” *pmoA* genes against our metagenomes. Notably, a branch of *pmoA* consists only of metagenome rhizome sequences, and these sequences are less than 65% identical to any sequence in the nr database. It is not clear whether they are true *pmoA* genes or *pmoA*-homologous *amoA* (ammonia monooxygenase) genes, as they match to *Nitrosococcus* and methanotrophs almost equally. However, their adjacent *pmoB* components are more similar to methanotrophs than to *Nitrosococcus*, suggesting that these novel sequences are likely from an unidentified methanotroph group.

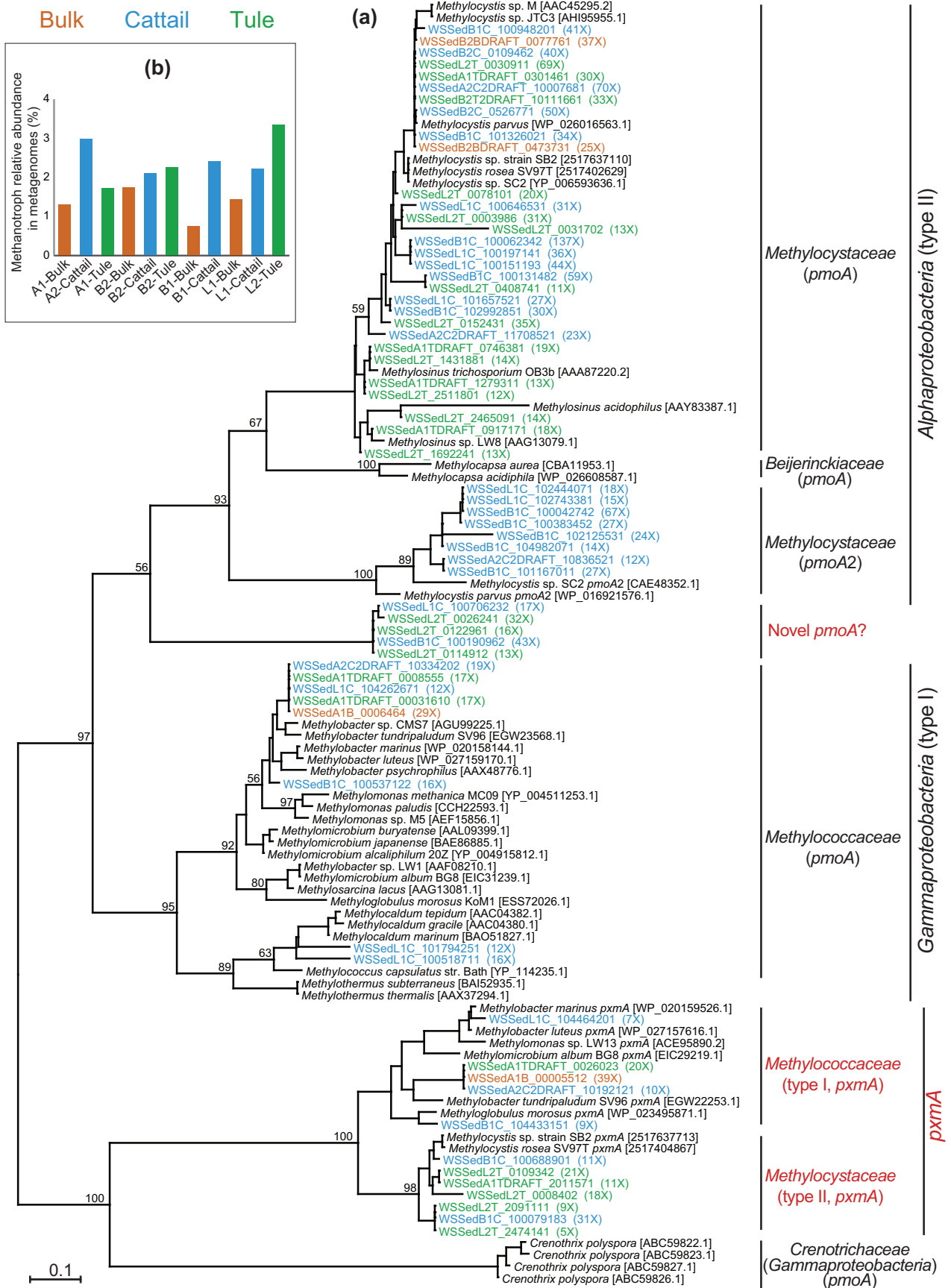
It was previously reported that all pMMO operons were organized as *pmoCAB*, whereas some gammaproteobacterial methanotrophs possess a novel *pmoA* gene in a *pmoABC* operon, in addition to the traditional *pmoA* gene in the *pmoCAB* operon (47). This *pmoA* was proposed to have an unknown function different from the traditional *pmoA* genes and was referred to as “*pxmA*.” A number of our wetland sequences were within the newly identified *Methylococcaceae pxmA* cluster, and they also have a *pmoABC* operon structure (if the operon is recovered), confirming their affiliation with *pxmA*. In addition, by searching reference methanotroph genomes, we also identified *Methylocystis* strain SB2 and *Methylocystis rosea* SV97T possessing such operon structures, and together with *Methylococcaceae*, they form a *pxmA* cluster, different from the traditional *pmoA* in either type I or II methanotrophs. A number of our wetland sequences were affiliated with these two *Methylocystis pxmA* sequences, and this finding suggests that this novel *pxmA* is present not only in type I as previously thought (47) but also in type II methanotrophs, although its function is still unclear.

The distribution of *pmoA* exhibited some patterns associated with sample types (Fig. 6a). Clearly, the number of *pmoA* sequences recovered from bulk peats is much lower than that from rhizomes. In addition, *pmoA* sequences affiliated with *Methylosinus* are mainly from tule rhizomes, whereas the *Methylocystaceae pmoA2* (an isozyme of *pmoA* in some *Methylocystis* genomes [48]) was found only in cattail rhizomes, suggesting some differential recruitments by the two plants.

As most methanotrophs possess pMMO (32), the abundance of methanotrophs was estimated by *pmoA* genes (see method details in Text S1E in the supplemental material) and ranged from 0.7 to 3.4% of the total community (Fig. 6b). In general, methanotrophs were present at higher abundances in the rhizomes than in the bulk peats within the same site. Overall, there is no correlation between methanotroph abundance and methanogen or methane production, suggesting that oxygen availability in the microenvironment is probably the limiting factor controlling methanotroph populations in this wetland. As we consider the bulk sediment to be anoxic, the presence of aerobic methanogens, although at low levels, may be due to the many fine roots in the sediment, allowing oxygen to penetrate peats surrounding these roots, therefore increasing the microheterogeneity of the sediment.

We also constructed an *mmoX* phylogenetic tree (see Fig. S6 in

FIG 5 Diversity of *mcrA* genes and abundance of methanogens. (a) Phylogenetic tree of *mcrA*, including all sequences recovered from metagenome assemblies with lengths of >150 amino acids. Wetland sequences are labeled with colors indicative of different sample sites, and their fold coverage in metagenomes is indicated in the parentheses. The accession numbers of reference sequences are in brackets. (b) Relative abundance of methanogens in the total community estimated by *mcr* genes.



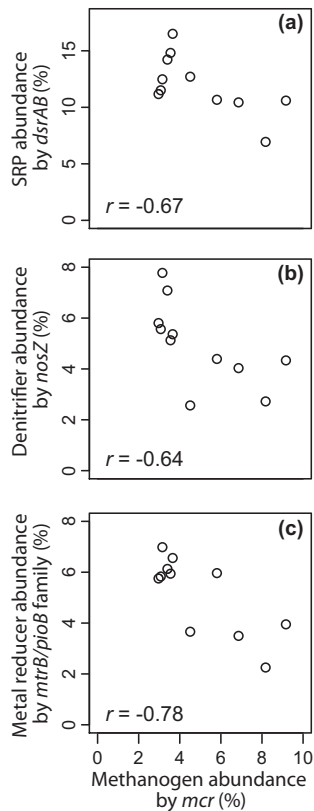


FIG 7 Relative abundances of sulfate-reducing prokaryotes (SRP) estimated by dissimilatory sulfite reductase genes (*dsrAB*) (a), denitrifiers by nitrous oxide reductase genes (*nosZ*) (b), and metal reducers by the multiheme *c*-type cytochrome-associated *mtrB/pioB* gene family (c) show negative correlations with methanogen abundance estimated by methyl coenzyme M reductase genes (*mcr*).

the supplemental material). As expected, fewer *mmoX* sequences were recovered from the wetland, and in particular, no *mmoX* sequences were obtained from bulk peats. About two-thirds of the wetland *mmoX* sequences are in the *Methylocystaceae* and *Methylococcaceae* families, and about one-third belong to *Beijerinckiaceae*, including members such as *Methylocella* and *Methyloferula*, which lack the *pmoA* genes in their genomes. Therefore, the above methanotroph abundance estimation by *pmoA* overlooked the contribution of *Beijerinckiaceae* methanotrophs, although they are minor based on the number and sequence coverage of their *mmoX* genes.

Abundance of anaerobic respiring populations. We estimated the abundances of sulfate reducers using the dissimilatory sulfite reductase genes (*dsrAB*) and of denitrifiers using nitrous oxide reductase genes (*nosZ*), and they ranged from 7% to 17% and from 3% to 8% of the total community, respectively (Fig. 7a and b; see also Text S1E in the supplemental material for method details). We used the *mtrB/pioB* gene family to estimate metal reducers that possess *mtrB*, encoding an outer membrane protein associated with multiheme *c*-type cytochromes involved in extra-

cellular electron transfer in dissimilatory metal reduction (49, 50), acknowledging that this might have led to overestimation of *mtrB*-containing metal reducers, because this gene family is also found in a few iron-oxidizing bacteria (51). In addition, metal reducers using other mechanisms were not evaluated in our study, partly because their metal reduction genetic machinery is less well understood. Overall, the inlet site had the highest abundances of denitrifiers, sulfate reducers, and metal reducers, and the interior site had the lowest abundances of these guilds (see Fig. S7). Correlations were observed between nitrate concentration and denitrifier relative abundance ($r = 0.78$), between the reduced Fe and Mn and metal reducers ($r = -0.93$), and between sulfate and sulfate reducers ($r = 0.96$) (see Fig. S7), indicating a strong relationship between site chemistry and corresponding microbial populations. Interestingly, populations of anaerobic respiring populations were positively correlated with each other (average $r = 0.67$), suggesting that these guilds may not be in direct competition.

In contrast, methanogen abundance was negatively correlated with the abundances of sulfate reducers ($r = -0.67$ [Fig. 7a]), denitrifiers ($r = -0.64$ [Fig. 7b]), and metal reducers ($r = -0.78$ [Fig. 7c]), respectively, suggesting that these anaerobic respiration processes may serve as electron sinks diverting electrons from methanogenesis in this wetland. These respiration processes are thermodynamically more favorable than methanogenesis and are expected to outcompete methanogenesis (52). Furthermore, sulfate reducers have higher affinities for H_2 and acetate than do methanogens (53, 54), and iron reducers also have a higher affinity for acetate and compete effectively with methanogens in wetland surface sediments (55). In addition, denitrification intermediates such as nitrite and nitric oxide may be toxic to methanogens (56, 57). Therefore, these electron acceptors, if present at sufficient concentrations, can both inhibit methanogenesis and suppress methanogen abundance, thus mitigating the global warming potential from wetlands.

Although wetland restoration recovers valuable ecosystem services, restoration projects need to be carefully designed and managed to minimize GHG emissions. Our results indicate that methanogens were present throughout this wetland, ranging from 2% to 10% of the total community, and redox conditions favoring peat accretion also encouraged methanogens and methane emission. Therefore, carbon sequestration and storage as peat need to be carefully balanced with GHG emission throughout the management of the restoration. In general, net GHG emission may depend on the interplay of a number of factors, including climate, soil type, plant species, hydrology, and water chemistry. From the perspective of the microbial contribution to GHG flux, increasing the water inflow rate to increase electron acceptor influxes or draining the wetland intermittently to reoxidize reduced electron acceptors may be promising in mitigating CH_4 emissions. In addition, as methanogenesis was more significant at the backwater sites, which experienced less water flow and less influx of electron acceptors, changing the wetland hydraulic design to minimize backwater areas might be effective to reduce CH_4 emission but

FIG 6 Diversity of *pmoA* genes and abundance of methanotrophs. (a) Phylogenetic tree of *pmoA*, including sequences recovered from metagenome assemblies with lengths of >80 amino acids. Wetland sequences were labeled with colors indicative of different sample types, and their fold coverage in metagenomes was indicated in the parentheses. The accession numbers of reference sequences are in brackets. (b) Relative abundance of methanotrophs in the total community estimated by *pmoA* genes.

must be evaluated against benefits of plant productivity and habitat quality.

In summary, the differences in microbial community composition and functional profiles reveal complex interactions among functional guilds and among wetland plants, microorganisms, and their environment. Analyses of 16S rRNA and functional genes showed distribution patterns associated with biogeochemistry and indicated microspatial heterogeneity of wetland sediments. Phylogeny of marker genes revealed a diversity of major methane-producing and -consuming populations and discovered novel diversity within methanotrophs. Quantitative comparative analyses of shotgun sequence data reveal the competition with and inhibition of methanogens by anaerobic respiring microorganisms without biases introduced by cultivation or PCR amplification and provided molecular evidence explaining the spatial variations in biogeochemistry and methane production. This information is useful in planning and operating wetland restoration projects in order to reduce CH₄ emission to the atmosphere and maintain the carbon storage potential of restored wetlands. Based on these findings, more specific studies can be carried out to evaluate the impact of wetland water chemistry and hydrology on CH₄ emission and carbon sequestration before large-scale restoration projects are implemented.

MATERIALS AND METHODS

Site description. A USGS pilot-scale wetland restoration project, located on Twitchell Island in the Sacramento-San Joaquin River Delta, CA, USA (121.65°W, 38.11°N), was constructed in 1997 by permanently flooding two adjacent agricultural plots, each about 3 ha, with standing water depths of 25 cm (west pond) and 55 cm (east pond), respectively (see Fig. S1 in the supplemental material). Details about the wetland construction were described previously (7). The water table was maintained by piping in fresh water from the surrounding San Joaquin River, continuously entering the wetlands from inlets, and flowing out through weirs near the middle of the north edge of each pond (see Fig. S1). The river water was a source of sulfate, phosphate, nitrate, and iron, ranging from 6 to 35 mg SO₄²⁻/liter, 0.1 to 0.4 mg PO₄³⁻/liter, 0.1 to 1.0 mg NO₃⁻/liter, and 0.2 to 0.5 mg Fe/liter, respectively (10). Two emergent marsh species, cattails (*Typha* spp.) and tules (*Schoenoplectus acutus*), are the primary vegetation that established postrestoration (58).

Sample collection and pore water chemical analysis. We collected belowground samples from three sites with various proximities to the inlets: sites A (inlet), B (transitional), and L (interior) in February (winter, nongrowing season for wetland vegetation) and sites A (inlet), B (transitional), and C (interior) in August (growing season) during 2011 (see Fig. S1 in the supplemental material). We used a custom-made Hargis corer (59) to collect duplicate cores from each site (e.g., cores A1 and A2 from site A). Each core, about 10 cm in diameter and 25 cm in length, was split into two sections by depth, 0 to 12 cm and 12 to 25 cm belowground, respectively. From each section, we collected three types of biomass samples, including bulk peat (mostly unidentifiable decomposed organic material), cattail rhizomes, and tule rhizomes, if available. Surface soil samples from the adjacent cornfield, to approximate soil prior to the restoration, were collected as a reference point. Samples for DNA extraction were immediately frozen on dry ice upon collection. For the February collection, in parallel with preserving samples for microbial community analysis, a subsample was taken from each sample, placed on ice, and transported immediately to the laboratory for anoxic incubation (see below). Temperature, pH, and dissolved oxygen (DO) were measured on site with YSI probes (model 6920-v2). Pore water was collected by syringe from each site at three depths, 0 cm (at the standing water-peat interface), 5 cm, and 20 cm belowground, respectively, and then filtered through 0.45- μ m filters for soluble chemicals. For February sampling, two sets of

pore water subsamples were collected. One set was directly collected into sealed serum bottles, and the other set was preserved in sulfuric acid (H₂SO₄) to a concentration of 0.2% by volume in sealed serum bottles. Both sets were immediately frozen on dry ice for later testing by the Aqueous Chemistry Laboratory at Lawrence Berkeley National Laboratory. Sulfuric acid-preserved pore water samples were used for total iron (Fe) and manganese (Mn) measurements using inductively coupled plasma mass spectrometry (ICP-MS). The other set of pore water samples was used for nitrate, nitrite, phosphate, sulfate, chloride, and acetate anion measurements using ion chromatography and for ammonia measurement using the salicylate method (Hach, Loveland, CO). For August sampling, pore water samples were directly collected into sealed serum bottles and immediately frozen on dry ice for the above-described tests by the Aqueous Chemistry Laboratory at Lawrence Berkeley National Laboratory. Ammonia and nitrite concentrations were mostly below their detection limits (0.05 mg/liter and 0.1 mg/liter, respectively), and acetate concentrations were below 1 mg/liter and in many cases below the detection limit (0.1 mg/liter).

Laboratory incubation. Fresh wet samples (6.3 \pm 4.0 g by dry weight) collected in February were placed into 480-ml glass jars fitted with airtight lids. Water from sites A, B, and L was used to submerge samples collected from the corresponding site; air and water volumes of the jars were recorded. Jars containing samples and water blanks were flushed with N₂ and incubated in the dark at 10°C for 12 days. Gas sampling was achieved through a bulkhead union sealed with silicone and fitted with a three-way stopcock. On days 7 and 12, headspace gas was sampled with a syringe and analyzed for CH₄ concentration using a micro-GC P200 gas chromatograph (Agilent Technologies Inc., Santa Clara, CA). CH₄ production was calculated using the ideal gas law, corrected for CH₄ equilibration with water using Henry's law, and then normalized by sample dry weights, which were determined by oven-drying the sample to a consistent mass at 65°C. CH₄ production rates from the two time points were averaged. Duncan's new multiple range test with a confidence level of 0.10 was performed using the R "agricolae" package to evaluate the statistical significance of differences among the three sites.

On-site CH₄ flux. For August sampling, on-site GHG flux was measured using a series of stationary whole-plant chambers deployed at sites A, B, and C, with duplicate chambers at each site. The chambers, with different heights customized to best accommodate vegetation heights (280 to 412 cm tall, 1-m² area), were constructed of polyvinyl chloride (PVC) pipes and enclosed by large Mylar sleeves, which moved freely over the PVC structures. Chambers were constructed as non-steady-state, nonvented flowthrough systems where air inside the chambers was cycled through a fast greenhouse gas analyzer (FGGA; Los Gatos Research Inc.) to measure CH₄ concentration at a frequency of 1 Hz. Each site was equipped with one FGGA, and a manifold alternated air samples between the two chambers in 1-min intervals for 16 min at the beginning of each hour, generating eight 1-min intervals from each chamber. Prior to the first measurement in each hour, the Mylar sleeves were lowered, allowing a short period (usually less than a minute) for the chamber environment to equilibrate. The sleeves then remained lowered and maintained consistent contact with the water surface for the duration of the 16-min measurement period. Between each 1-min interval, ambient atmospheric air was cycled through the FGGA to provide a clear reference delimiting the two chambers at each site. At the end of each 16-min sampling period, sleeves were raised and the chambers remained open until the next hour. Within each 1-min interval, concentrations (parts per million) were converted to number of moles using the ideal gas law and fluxes were then calculated as a change in GHG mass per square meter of covered area versus time. As CH₄ flux exhibited a diurnal pattern with peaks around midmorning to noon (data not shown), the results from the eight intervals during the 16-min period at noon in two consecutive days from the two replicate chambers were averaged to indicate noon flux for each site.

DNA extraction. About 1.5 g of peat sample (by wet weight) was used in each DNA extraction. Phosphate-buffered saline solution (PBS; 1×, pH 7.2) was added to each sample and vigorously mixed at the maximal speed on a Vortex-Genie 2 vortex (USA Scientific, Inc., Orlando, FL) for at least 5 min to elute microbial biomass from plant tissues or detritus. Large pieces of plant material were removed with pipette tips, and the remaining cell suspension was transferred to a new tube and centrifuged at $5,000 \times g$ at 4°C for 5 min to collect cell pellets. DNA was extracted from cell pellets by using the PowerLyzer PowerSoil DNA isolation kit (Mo Bio Laboratories, Inc., Carlsbad, CA) according to the manufacturer's instructions. Duplicate DNA extractions were performed on each sample, and both duplicates were individually used for 16S rRNA gene sequencing. For metagenome sequencing, multiple DNA extractions were performed for each sample and pooled to obtain sufficient DNA for shotgun library construction.

16S rRNA gene sequencing and microbial community analysis. Pyrosequencing of PCR-amplified V8 regions of 16S rRNA genes was used to generate microbial community profiles. The 454 adaptor-added 16S rRNA gene primer set, 926Fw (5' to 3', AAACYAAAKGAATTGRCGG) and 1392R (5' to 3', ACGGGCGGTGTGTRC), was used to amplify the V6-V8 region, with 5-bp bar codes incorporated into the reverse primer to allow sample multiplexing. PCR amplicons were sequenced by the DOE Joint Genome Institute, using the Roche 454 GS FLX titanium technology as previously described (60). Sequences were analyzed through the Pyro-Tagger computational pipeline (<http://pyrotagger.jgi-psf.org>) for sequence trimming, clustering into operational taxonomic units (OTUs) based on 97% sequence identity, and taxonomic assignment by BLASTn against the Greengenes database (61). For sequence trimming with Pyro-Tagger, based on the per-base sequence quality graph, quality scores did not start to drop until after the first 200 bases, and therefore, we trimmed all sequences to a uniform length to contain only the first 200 bases. Singletons and potential chimeras were removed to minimize the impact of PCR artifacts. This primer set amplifies 16S rRNA sequences from most bacteria and archaea as well as 18S rRNA sequences from eukaryotes; eukaryote sequences, both nuclear and organelle, made up 0.1% to 48.5% of reads per sample and were excluded from downstream analysis. To calculate alpha diversity, we used the R "phyloseq" package to rarefy all samples to the size of the smallest data set, 1,738 sequences, before calculating the Shannon diversity index. For beta diversity, nonmetric multidimensional scaling (NMDS) analysis was conducted using the software package PRIMER (v6.1.9), with a Bray-Curtis similarity matrix based on the relative abundance of OTUs. Analysis of similarities (ANOSIM) was used to assess the community composition differences among the classified sample groups. The ANOSIM *R* statistic value of "0" indicates completely random grouping, and "1" indicates a complete separation among sample groups. In addition, permutation multivariate analysis of variance (PerMANOVA) was also performed to evaluate statistical significance of differences among classified sample groups using the R "vegan" package, with Bray-Curtis distance and 1,000 permutations. OTUs that contributed to >0.1% of the dissimilarity between two sample groups were identified by the similarity percent (SIMPER) test. Student *t* tests were performed on these identified OTUs to determine the statistically over- or underrepresented (*P* value of <0.05) OTUs between the two groups of samples. Correspondence analysis was also conducted to study community composition patterns and the correlation with environmental variables using Canoco for Windows (v4.5.3). In addition, Spearman correlation was generated between each pair of OTUs based on their relative abundance among all samples, with *P* values adjusted using the false discovery rate (FDR) (Benjamini-Hochberg) method (62) for multiple hypothesis testing using the R "Hmisc" package, and the correlation matrix was used for network analysis with Cytoscape (v3.0.2).

Metagenome sequencing, assembly, and annotation. For metagenomic analysis, we selected a total of 11 representative samples collected in February, including a spectrum of sample sites and types. Shotgun

libraries were constructed with insert sizes of ~250 bp and sequenced on the Illumina HiSeq 2000 platform to generate paired-end (2×150 -bp) reads. One lane of HiSeq sequences was generated for each library, with raw sequence yields of 50 to 60 Gbp from each lane. Raw reads were trimmed using a minimum quality cutoff of Q10 and assembled largely as described in the work of Scholz et al. (63). Trimmed, paired-end reads from each sample were first assembled using SOAPdenovo v1.05 (<http://soap.genomics.org.cn/soapdenovo.html>) with default settings (-d 1 and -R) at different kmer sizes (85, 89, 93, 97, 101, and 105, respectively). Contigs generated by each assembly (a total of six contig sets from the six kmer sizes) were merged using in-house Perl scripts as following. Contigs were first dereplicated and sorted into two pools based on length. Contigs of <1,800 bp were assembled using Newbler (Life Technologies, Carlsbad, CA) to generate larger contigs (-tr, -rip, -mi 98, -ml 80). All assembled contigs of >1,800 bp, as well as the contigs generated from the Newbler assembly, were combined and merged using minimus2 (-D MINID=98 -D OVERLAP=80) (AMOS: <http://sourceforge.net/projects/amos>). The average fold coverage (or read depth) of each contig was estimated by mapping all reads back to the final assembly using BWA (v1.2.2) (64). The metagenome sequences, including both assembled contigs and reads not mapped to the assembly (i.e., unassembled reads), were uploaded to the Integrated Microbial Genomes with Microbiomes (IMG/M) database (img.jgi.doe.gov/m) for gene prediction and functional annotation (65). The IMG/M taxon identifiers (IDs) are 3300000030, 3300000090, 3300000091, 3300000092, 3300000093, 3300000094, 3300000100, 3300000108, 3300000786, 3300000854, and 3300000894 for the 11 metagenomes, respectively. The average read depth for each contig was also uploaded to IMG/M as an estimator of the abundance of the population from which the contig was derived.

Metagenome comparison. We used gene-centric analysis of shotgun metagenome data to reveal differences in community functional profiles (66). We compared metagenomes based on the functional unit of COGs and on Pfams in cases where COGs were not available or not specific for a function. The abundance of a functional gene family was estimated by the number of recovered genes belonging to this gene family adjusted (multiplied) by the average read depth of the corresponding contig to account for the population abundance. To compare among all metagenomes, we formed a combined average metagenome from the 11 metagenomes as a common reference. The odds ratio of a COG (or Pfam) between an individual metagenome and the combined average metagenome was used to compare gene abundance across samples.

Phylogenetic tree construction. Multiple sequence alignment was generated with MUSCLE (67). A maximum likelihood phylogenetic tree was constructed using PhyML 3.0 (68), with the LG substitution model (69) and gamma distribution parameter estimated by PhyML. Bootstrap values were calculated based on 100 replicas. The tree was visualized with Dendroscope (v3.2.10) with midpoint root.

Estimation of relative abundance of functional populations. The abundance of a functional population was estimated by marker genes in the corresponding pathway, and the total microbial community was estimated by the average from a total of 37 COGs representing single-copy housekeeping genes. Because the detection frequency of a gene is highly dependent on its expected full length, especially in short read data, we performed normalization on COG or Pfam gene abundance by its expected full length (the consensus length of a COG or the average domain length for a Pfam). The length-normalized abundance of a functional marker gene family was then compared against the average of length-normalized abundance of the 37 housekeeping COGs to approximate the percentage of genomes possessing that function (i.e., relative abundance of a functional population). Method details and relevant discussion are available in Text S1 in the supplemental material.

Nucleotide sequence accession numbers. Raw sequence reads of the V8 regions of 16S rRNA genes were submitted to the Sequence Read Archive (SRA) under accession no. SRP003022. Raw sequence reads for

metagenomes were submitted to the SRA with accession numbers SRP010671, SRP010730, SRP010738, SRP010741, SRP010747, SRP010748, SRP010751, SRP010862, SRP010870, and SRP011309.

SUPPLEMENTAL MATERIAL

Supplemental material for this article may be found at <http://mbio.asm.org/lookup/suppl/doi:10.1128/mBio.00066-15/-/DCSupplemental>.

Text S1, DOCX file, 1.8 MB.
Figure S1, PDF file, 0.5 MB.
Figure S2, PDF file, 0.1 MB.
Figure S3, PDF file, 0.2 MB.
Figure S4, PDF file, 0.2 MB.
Figure S5, PDF file, 2.4 MB.
Figure S6, PDF file, 0.2 MB.
Figure S7, PDF file, 0.2 MB.
Table S1, PDF file, 0.1 MB.
Table S2, PDF file, 0.8 MB.

ACKNOWLEDGMENTS

We thank the production and sequence analysis teams at JGI for sequencing and bioinformatic support; Scott Clingenpeel at JGI, Maggi Kelly, Sarah Lewis, and Lisa Schile at University of California, Berkeley, and Kristin Byrd at U.S. Geological Survey for help with sample collection; USGS staff support, including Travis von Dessonneck and Kathryn Keating, for GHG data collection and interpretation over 24-h periods; April Van Hise at LBNL for pore water analyses; Shane Canon at NERSC for assistance with annotation; and Trina McMahon at University of Wisconsin Madison for feedback on the manuscript.

This project was funded by the DOE Early Career Research Program, grant no. KP/CH57/1; the DOE JGI Community Sequencing Program; and the USGS Climate and Land Use Change Program. The work conducted by the U.S. Department of Energy Joint Genome Institute is supported by the Office of Science of the U.S. Department of Energy under contract no. DE-AC02-05CH11231.

The authors declare no conflict of interest.

REFERENCES

- Mitsch WJ, Gosselink JG. 2007. Wetlands, 4th ed. John Wiley & Sons, Hoboken, NJ.
- Mitsch WJ, Bernal B, Nahlik AM, Mander UI, Zhang L, Anderson CJ, Jørgensen SE, Brix H. 2013. Wetlands, carbon, and climate change. *Landscape Ecol* 28:583–597. <http://dx.doi.org/10.1007/s10980-012-9758-8>.
- Sleeter BM, Sohl TL, Loveland TR, Auch RF, Acevedo W, Drummond MA, Saylor KL, Stehman SV. 2013. Land-cover change in the conterminous United States from 1973 to 2000. *Glob Environ Change* 23:733–748. <http://dx.doi.org/10.1016/j.gloenvcha.2013.03.006>.
- Thompson J. 1957. The settlement geography of the Sacramento-San Joaquin Delta, California. Ph.D. thesis. Stanford University, Stanford, CA.
- Deverel SJ, Rojstaczer S. 1996. Subsidence of agricultural lands in the Sacramento-San Joaquin Delta, California: role of aqueous and gaseous carbon fluxes. *Water Resour Res* 32:2359–2367. <http://dx.doi.org/10.1029/96WR01338>.
- Drexler JZ, Fontaine CS, Deverel SJ. 2009. The legacy of wetland drainage on the remaining peat in the Sacramento-San Joaquin Delta, California, USA. *Wetlands* 29:372–386. <http://dx.doi.org/10.1672/08-97.1>.
- Miller RL, Fram MS, Fujii R, Wheeler G. 2008. Subsidence reversal in a re-established wetland in the Sacramento-San Joaquin Delta, California, USA. *San Francisco Estuary Watershed Sci* 6:1–20. <http://escholarship.org/uc/item/5j76502x>
- Denman KL, Brasseur G, Chidthaisong A, Ciais P, Cox PM, Dickinson RE, Hauglustaine D, Heinze C, Holland E, Jacob D, Lohmann U, Ramachandran S, Dias PLDS, Wofsy SC, Zhang X. 2007. Couplings between changes in the climate system and biogeochemistry, p 499–587. *In* Solomon S, Qin D, Manning M, Chen Z, Marquis M, Averyt KB, Tignor M, Miller HL. (ed), *Climate change 2007: the physical science basis. Contribution of Working Group I to the Fourth Assessment Report of the Intergovernmental Panel on Climate Change*. Cambridge University Press, Cambridge, United Kingdom.
- Whiting GJ, Chanton JP. 2001. Greenhouse carbon balance of wetlands: methane emission versus carbon sequestration. *Tellus B* 53:521–528. <http://dx.doi.org/10.1034/j.1600-0889.2001.530501.x>.
- Miller RL. 2011. Carbon gas fluxes in re-established wetlands on organic soils differ relative to plant community and hydrology. *Wetlands* 31:1055–1066. <http://dx.doi.org/10.1007/s13157-011-0215-2>.
- Kayranli B, Scholz M, Mustafa A, Hedmark Å. 2010. Carbon storage and fluxes within freshwater wetlands: a critical review. *Wetlands* 30:111–124. <http://dx.doi.org/10.1007/s13157-009-0003-4>.
- Laanbroek HJ. 2010. Methane emission from natural wetlands: interplay between emergent macrophytes and soil microbial processes. A mini-review. *Ann Bot* 105:141–153. <http://dx.doi.org/10.1093/aob/mcp201>.
- Le Mer J, Roger JP. 2001. Production, oxidation, emission and consumption of methane by soils: a review. *Eur J Soil Biol* 37:25–50. [http://dx.doi.org/10.1016/S1164-5563\(01\)01067-6](http://dx.doi.org/10.1016/S1164-5563(01)01067-6).
- Bridgman SD, Cadillo-Quiroz H, Keller JK, Zhuang Q. 2013. Methane emissions from wetlands: biogeochemical, microbial, and modeling perspectives from local to global scales. *Glob Chang Biol* 19:1325–1346. <http://dx.doi.org/10.1111/gcb.12131>.
- Carpenter K, Snyder D, Duff J, Triska F, Lee K, Avanzino R, Sobieszcyk S. 2009. Hydrologic and water-quality conditions during restoration of the Wood River wetland, upper Klamath River Basin, Oregon, 2003–05: U.S. Geological Survey Scientific Investigations Report 2009-5004. U.S. Department of the Interior, U.S. Geological Survey, Reston, VA.
- Reddy KR, DeLaune RD. 2008. Biogeochemistry of wetlands: science and applications. CRC Press, Taylor and Francis Group, Boca Raton, FL.
- Rivière D, Desvignes V, Pelletier E, Chaussonnerie S, Guermazi S, Weissenbach J, Li T, Camacho P, Sghir A. 2009. Towards the definition of a core of microorganisms involved in anaerobic digestion of sludge. *ISME J* 3:700–714. <http://dx.doi.org/10.1038/ismej.2009.2>.
- Roberts DG, McComb AJ. 1984. The structure and continuity of the lacunar system of the seagrass *Halophila ovalis* (R. Br.) Hook f. (Hydrocharitaceae). *Aquat Bot* 18:377–388.
- Caffrey JM, Kemp WM. 1991. Seasonal and spatial patterns of oxygen production, respiration and root-rhizome release in *Potamogeton perfoliatus* L. and *Zostera marina* L. *Aquat Bot* 40:109–128. [http://dx.doi.org/10.1016/0304-3770\(91\)90090-R](http://dx.doi.org/10.1016/0304-3770(91)90090-R).
- Walker TS, Bais HP, Grotewold E, Vivanco JM. 2003. Root exudation and rhizosphere biology. *Plant Physiol* 132:44–51. <http://dx.doi.org/10.1104/pp.102.019661>.
- Ström L, Ekberg A, Mastepanov M, Røjle Christensen T. 2003. The effect of vascular plants on carbon turnover and methane emissions from a tundra wetland. *Glob Change Biol* 9:1185–1192. <http://dx.doi.org/10.1046/j.1365-2486.2003.00655.x>.
- Bais HP, Weir TL, Perry LG, Gilroy S, Vivanco JM. 2006. The role of root exudates in rhizosphere interactions with plants and other organisms. *Annu Rev Plant Biol* 57:233–266. <http://dx.doi.org/10.1146/annurev.arplant.57.032905.105159>.
- Liu Y, Whitman WB. 2008. Metabolic, phylogenetic, and ecological diversity of the methanogenic archaea. *Ann N Y Acad Sci* 1125:171–189. <http://dx.doi.org/10.1196/annals.1419.019>.
- Bräuer U, Cadillo-Quiroz H, Ward RJ, Yavitt JB, Zinder SH. 2011. *Methanoregula boonei* gen. nov., sp. nov., an acidiphilic methanogen isolated from an acidic peat bog. *Int J Syst Evol Microbiol* 61:45–52. <http://dx.doi.org/10.1099/ijs.0.021782-0>.
- Yashiro Y, Sakai S, Ehara M, Miyazaki M, Yamaguchi T, Imachi H. 2011. *Methanoregula formicica* sp. nov., a methane-producing archaeon isolated from methanogenic sludge. *Int J Syst Evol Microbiol* 61:53–59. <http://dx.doi.org/10.1099/ijs.0.014811-0>.
- Jetten M, Stams AJM, Zehnder AJB. 1992. Methanogenesis from acetate: a comparison of the acetate metabolism in *Methanotheroxobacterium* and *Methanosarcina* spp. *FEMS Microbiol Lett* 88:181–198. [http://dx.doi.org/10.1016/0378-1097\(92\)90802-U](http://dx.doi.org/10.1016/0378-1097(92)90802-U).
- Castro HF, Williams NH, Ogram A. 2000. Phylogeny of sulfate-reducing bacterial. *FEMS Microbiol Ecol* 31:1–9.
- Hoor AT-T. 1975. A new type of thiosulphate oxidizing, nitrate reducing microorganism: *Thiomicrospira denitrificans* sp. nov. *Neth J Sea Res* 9:344–350.
- Beller HR, Chain PS, Letain TE, Chakicherla A, Larimer FW, Richardson PM, Coleman MA, Wood AP, Kelly DP. 2006. The genome sequence of the obligately chemolithoautotrophic, facultatively anaerobic bacterium *Thiobacillus denitrificans*. *J Bacteriol* 188:1473–1488. <http://dx.doi.org/10.1128/JB.188.4.1473-1488.2006>.
- Lovley DR, Ueki T, Zhang T, Malvankar NS, Shrestha PM, Flanagan

- KA, Aklujkar M, Butler JE, Giloteaux L, Rotaru A.-E, Holmes DE, Franks AE, Orellana R, Rizzo C, Nevin KP, Robert KP. 2011. *Geobacter*: the microbe electric's physiology, ecology, and practical applications. *Adv Microb Physiol* 59:1–100. <http://dx.doi.org/10.1016/B978-0-12-387661-4.00004-5>.
31. Hanson RS, Hanson TE. 1996. Methanotrophic bacteria. *Microbiol Rev* 60:439–471.
 32. McDonald IR, Bodrossy L, Chen Y, Murrell JC. 2008. Molecular ecology techniques for the study of aerobic methanotrophs. *Appl Environ Microbiol* 74:1305–1315. <http://dx.doi.org/10.1128/AEM.02233-07>.
 33. Cadillo-Quiroz H, Yavitt JB, Zinder SH, Thies JE. 2010. Diversity and community structure of archaea inhabiting the rhizosphere of two contrasting plants from an acidic bog. *Microb Ecol* 59:757–767. <http://dx.doi.org/10.1007/s00248-009-9628-3>.
 34. Kiener A, Leisinger T. 1983. Oxygen sensitivity of methanogenic bacteria. *Syst Appl Microbiol* 4:305–312. [http://dx.doi.org/10.1016/S0723-2020\(83\)80017-4](http://dx.doi.org/10.1016/S0723-2020(83)80017-4).
 35. Angel R, Matthies D, Conrad R. 2011. Activation of methanogenesis in arid biological soil crusts despite the presence of oxygen. *PLoS One* 6:e20453. <http://dx.doi.org/10.1371/journal.pone.0020453>.
 36. Grosskopf R, Stubner S, Liesack W. 1998. Novel euryarchaeotal lineages detected on rice roots and in the anoxic bulk soil of flooded rice microcosms. *Appl Environ Microbiol* 64:4983–4989.
 37. Hershberger KL, Barns SM, Reysenbach A.-L, Dawson SC, Pace NR. 1996. Wide diversity of Crenarchaeota. *Nature* 384:420. <http://dx.doi.org/10.1038/384420a0>.
 38. Sekiguchi Y. 2006. Yet-to-be cultured microorganisms relevant to methane fermentation processes. *Microb Environ* 21:1–15. <http://dx.doi.org/10.1264/jisme.2.21.1>.
 39. Philippot L, Hallin S, Börjesson G, Baggs EM. 2009. Biochemical cycling in the rhizosphere having an impact on global change. *Plant Soil* 321: 61–81. <http://dx.doi.org/10.1007/s11104-008-9796-9>.
 40. Chanton JP, Whiting GJ, Blair NE, Lindau CW, Bollich PK. 1997. Methane emission from rice: stable isotopes, diurnal variations, and CO₂ exchange. *Global Biogeochem Cycles* 11:15–27. <http://dx.doi.org/10.1029/96GB03761>.
 41. Schütz H, Seiler W, Conrad R. 1989. Processes involved in formation and emission of methane in rice paddies. *Biogeochemistry* 7:33–53. <http://dx.doi.org/10.1007/BF00000896>.
 42. Logares R, Sunagawa S, Salazar G, Cornejo-Castillo FM, Ferrera I, Sarmiento H, Hingamp P, Ogata H, de Vargas C, Lima-Mendez G, Raes J, Poulain J, Jaillon O, Wincker P, Kandels-Lewis S, Karsenti E, Bork P, Acinas SG. 2014. Metagenomic 16S rDNA Illumina tags are a powerful alternative to amplicon sequencing to explore diversity and structure of microbial communities. *Environ Microbiol* 16:2659–2671. <http://dx.doi.org/10.1111/1462-2920.12250>.
 43. Bowman JP, Sly LI, Nichols PD, Hayward AC. 1993. Revised taxonomy of the methanotrophs: description of *Methylobacter* gen. nov., emendation of *Methylococcus*, validation of *Methylosinus* and *Methylocystis* species, and a proposal that the family *Methylococcaceae* includes only the group I methanotrophs. *Int J Syst Bacteriol* 43:735–753.
 44. Dunfield PF, Yuryev A, Senin P, Smirnova AV, Stott MB, Hou S, Ly B, Saw JH, Zhou Z, Ren Y, Wang J, Mountain BW, Crowe MA, Weatherby TM, Bodelier PL, Liesack W, Feng L, Wang L, Alam M. 2007. Methane oxidation by an extremely acidophilic bacterium of the phylum Verrucomicrobia. *Nature* 450:879–882. <http://dx.doi.org/10.1038/nature06411>.
 45. Ettwig KF, Butler MK, Le Paslier D, Pelletier E, Mangenot S, Kuypers MM, Schreiber F, Dutilh BE, Zedelius J, de Beer D, Gloerich J, Wessels HJ, van Alen T, Luesken F, Wu ML, van de Pas-Schoonen KT, Op den Camp HJ, Janssen-Megens EM, Francoijs KJ, Stunnenberg H, Weissenbach J, Jetten MS, Strous M. 2010. Nitrite-driven anaerobic methane oxidation by oxygenic bacteria. *Nature* 464:543–548. <http://dx.doi.org/10.1038/nature08883>.
 46. Theisen AR, Ali MH, Radajewski S, Dumont MG, Dunfield PF, McDonald IR, Dedysh SN, Miguez CB, Murrell JC. 2005. Regulation of methane oxidation in the facultative methanotroph *Methylocella silvestris* BL2. *Mol Microbiol* 58:682–692. <http://dx.doi.org/10.1111/j.1365-2958.2005.04861.x>.
 47. Tavormina PL, Orphan VJ, Kalyuzhnaya MG, Jetten MS, Klotz MG. 2011. A novel family of functional operons encoding methane/ammonia monooxygenase-related proteins in gammaproteobacterial methanotrophs. *Environ Microbiol Rep* 3:91–100. <http://dx.doi.org/10.1111/j.1758-2229.2010.00192.x>.
 48. Baani M, Liesack W. 2008. Two isozymes of particulate methane monooxygenase with different methane oxidation kinetics are found in *Methylocystis* sp. strain sc2. *Proc Natl Acad Sci U S A* 105:10203–10208. <http://dx.doi.org/10.1073/pnas.0702643105>.
 49. Beliaev AS, Saffarini DA. 1998. *Shewanella putrefaciens* mtrB encodes an outer membrane protein required for Fe(III) and Mn(IV) reduction. *J Bacteriol* 180:6292–6297.
 50. Shi L, Squier TC, Zachara JM, Fredrickson JK. 2007. Respiration of metal (hydr)oxides by *Shewanella* and *Geobacter*: a key role for multihaem c-type cytochromes. *Mol Microbiol* 65:12–20. <http://dx.doi.org/10.1111/j.1365-2958.2007.05783.x>.
 51. Liu J, Wang Z, Belchik SM, Edwards MJ, Liu C, Kennedy DW, Merkle ED, Lipton MS, Butt JN, Richardson DJ, Zachara JM, Fredrickson JK, Rosso KM, Shi L. 2012. Identification and characterization of MtoA: a decaheme c-type cytochrome of the neutrophilic Fe(II)-oxidizing bacterium *Sideroxydans lithotrophicus* ES-1. *Front Microbiol* 3:37. <http://dx.doi.org/10.3389/fmicb.2012.00037>.
 52. Thauer RK, Kaster A.-K, Seedorf H, Buckel W, Hedderich R. 2008. Methanogenic archaea: ecologically relevant differences in energy conservation. *Nat Rev Microbiol* 6:579–591. <http://dx.doi.org/10.1038/nrmicro1931>.
 53. Lovley DR, Klug MJ. 1983. Sulfate reducers can outcompete methanogens at freshwater sulfate concentrations. *Appl Environ Microbiol* 45: 187–192.
 54. Kristjansson JK, Schönheit P. 1983. Why do sulfate-reducing bacteria outcompete methanogenic bacteria for substrates? *Oecologia* 60:264–266. <http://dx.doi.org/10.1007/BF00379530>.
 55. Roden EE, Wetzel RG. 2003. Competition between Fe(III)-reducing and methanogenic bacteria for acetate in iron-rich freshwater sediments. *Microb Ecol* 45:252–258. <http://dx.doi.org/10.1007/s00248-002-1037-9>.
 56. Klüber H, Conrad R. 1998. Effects of nitrate, nitrite, NO and N₂O on methanogenesis and other redox processes in anoxic rice field soil. *FEMS Microbiol Ecol* 25:301–318. [http://dx.doi.org/10.1016/S0168-6496\(98\)00011-7](http://dx.doi.org/10.1016/S0168-6496(98)00011-7).
 57. Klüber H, Conrad R. 1998. Inhibitory effects of nitrate, nitrite, NO and N₂O on methanogenesis by *Methanosarcina barkeri* and *Methanobacterium bryantii*. *FEMS Microbiol Ecol* 25:331–339. [http://dx.doi.org/10.1016/S0168-6496\(97\)00102-5](http://dx.doi.org/10.1016/S0168-6496(97)00102-5).
 58. Miller RL, Fujii R. 2010. Plant community, primary productivity, and environmental conditions following wetland re-establishment in the Sacramento-San Joaquin Delta, California. *Wetlands Ecol Manage* 18: 1–16. <http://dx.doi.org/10.1007/s11273-009-9143-9>.
 59. Hargis TG, Twilley RR. 1994. Improved coring device for measuring soil bulk-density in a Louisiana deltaic marsh. *J Sediment Res* 64:681–683. <http://dx.doi.org/10.1306/D4267E60-2B26-11D7-8648000102C1865D>.
 60. Engelbrekton A, Kunin V, Wrighton KC, Zvenigorodsky N, Chen F, Ochman H, Hugenholtz P. 2010. Experimental factors affecting PCR-based estimates of microbial species richness and evenness. *ISME J* 4:642–647. <http://dx.doi.org/10.1038/ismej.2009.153>.
 61. Kunin V, Engelbrekton A, Ochman H, Hugenholtz P. 2010. Wrinkles in the rare biosphere: pyrosequencing errors can lead to artificial inflation of diversity estimates. *Environ Microbiol* 12:118–123. <http://dx.doi.org/10.1111/j.1462-2920.2009.02051.x>.
 62. Benjamin Y, Hochberg Y. 1995. Controlling the false discovery rate: a practical and powerful approach to multiple testing. *J R Stat Soc B (Methodol)* 57:289–300.
 63. Scholz M, Lo CC, Chain PS. 2014. Improved assemblies using a source-agnostic pipeline for MetaGenomic assembly by merging (MeGAMerge) of contigs. *Sci Rep* 4:6480. <http://dx.doi.org/10.1038/srep06480>.
 64. Li H, Durbin R. 2009. Fast and accurate short read alignment with Burrows-Wheeler transform. *Bioinformatics* 25:1754–1760. <http://dx.doi.org/10.1093/bioinformatics/btp324>.
 65. Markowitz VM, Chen I-MA, Chu K, Szeto E, Palaniappan K, Pillay M, Ratner A, Huang J, Pagani I, Tringe S, Huntemann M, Billis K, Varghese N, Tennessen K, Mavromatis K, Pati A, Ivanova NN, Kyrpides NC. 2014. IMG/M 4 version of the integrated metagenome comparative analysis system. *Nucleic Acids Res* 42(D1):D568–D573. <http://dx.doi.org/10.1093/nar/gkt919>.
 66. Tringe SG, von Mering C, Kobayashi A, Salamov AA, Chen K, Chang HW, Podar M, Short JM, Mathur EJ, Detter JC, Bork P, Hugenholtz P,

- Rubin EM. 2005. Comparative metagenomics of microbial communities. *Science* 308:554–557. <http://dx.doi.org/10.1126/science.1107851>.
67. Edgar RC. 2004. MUSCLE: a multiple sequence alignment method with reduced time and space complexity. *BMC Bioinformatics* 5:113. <http://dx.doi.org/10.1186/1471-2105-5-113>.
68. Guindon S, Dufayard JF, Lefort V, Anisimova M, Hordijk W, Gascuel O. 2010. New algorithms and methods to estimate maximum-likelihood phylogenies: assessing the performance of PhyML 3.0. *Syst Biol* 59: 307–321. <http://dx.doi.org/10.1093/sysbio/syq010>.
69. Le SQ, Gascuel O. 2008. An improved general amino acid replacement matrix. *Mol Biol Evol* 25:1307–1320. <http://dx.doi.org/10.1093/molbev/msn067>.